Int. J. Electrochem. Sci., 13 **(2018)** 8645 – 8656, doi: 10.20964/2018.09.17

International Journal of
ELECTROCHEMICAL
SCIENCE
www.electrochemsci.org

Inhibition Effect and Adsorption Behavior of Two Imidazolium-based Ionic Liquids on X70 Steel in Sulfuric Acid Solution

Jinliang Zhang[1,2], *Lijing Zhang*[1,*], *Gang Tao*[1], *Nanxi Chen*[3]

[1] College of Safety Science and Engineering, Nanjing Tech University, Nanjing 210009, China
[2] School of Materials and Chemical Engineering, Ningbo University of Technology, Ningbo 315211, China
[3] School of Chemistry and Chemical Engineering, Chongqing University, Chongqing 400044, China
[*]E-mail: zhanglj_njtech@163.com

Received: 8 April 2018 / *Accepted:* 28 May 2018 / *Published:* 5 August 2018

In this work, two imidazolium-based ionic liquids with different chain lengths namely 1-allyl-3-ethylimidazolium bromide ([AEIM]Br) and 1-allyl-3-hexylimidazolium bromide ([AHIM]Br) respectively, were researched on corrosion of X70 steel in 0.5 M sulphuric acid. The corrosion resistance ability was tested by electrochemical methods including the electrochemical impedance spectroscopy (EIS) and potentiodynamic polarization measurement. Results showed that [AHIM]Br have a better inhibition ability than [AEIM]Br. Scanning electron microscope (SEM) was utilized to further analysis the appearance of steel surface. Furthermore, the inhibition mechanism of two inhibitors was analyzed by adsorption isotherm study and molecular dynamics (MD) simulation. The experimental and theoretical results are consistent and the adsorption of the two inhibitors on steel surface belongs to mixed type of chemisorption and physisorption.

Keywords: Corrosion Inhibitor; Adsorption; X70 steel; EIS; Molecular Dynamics Simulation.

1. INTRODUCTION

Inhibitors are compounds that control and suppress reactions between a metal and its surrounding solution when adding to the medium in small quantities [1]. The most effective inhibitors are organics containing the heteroatoms (N, S, O and P) in a conjugated system, which act as active centers for their interaction with metal surface [2-7]. Organic inhibitors have been widely reported on corrosion inhibition for metal [8-10]. However, most of these inhibitors used towards steel corrosion in acidic media are toxic, volatile and expensive, causing a lot of pollution to the environment. Therefore,

attempts have been performed to find eco-friendly corrosion inhibitors for metals in recent years [11-13].

Ionic liquids (ILs) are molten salts, which are composed of organic cations and different anions, with melting points at or below ambient room temperature [14]. For the past few years, ILs have been proposed as green inhibitors to control metal corrosion in acid media [14]. In this work, two imidazolium-based ILs, 1-allyl-3-ethylimidazolium bromide ([AEIM]Br) and 1-allyl-3-hexylimidazolium bromide ([AHIM]Br) are explored as promising corrosion inhibitors of X70 steel, which is not reported before. For this investigation, the aim is to explore the effect of different chain length on inhibition ability of these compounds. The inhibition performance was investigated by electrochemical methods, weight loss experiment, and scanning electron microscope (SEM). The theoretical calculation and adsorption isotherm study were furtherly used to give evidence to adsorption mechanism.

2. EXPERIMENTAL

2.1. Sample and solution preparation

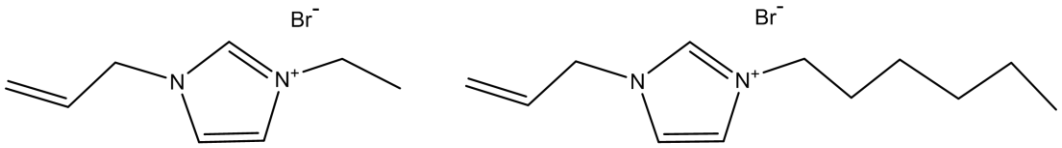

[AEIM]Br [AHIM]Br

Figure 1. The molecular structures of two investigated compounds

The composition (wt %) of the X70 steel specimen are as follows: C (0.06), Mn (1.52), Si (0.18), Cr (0.031), Cu (0.14), Ti (0.014), Ni (0.11), Mo (0.16), and remaining Fe. The steel was cut into coupons of 3 cm × 2 cm × 1 cm for weight loss test, and 1 cm × 1 cm × 1 cm for electrochemical experiment with an exposed area of 1 cm^2. Emery papers with 400-2000 grades were used to remove the oxide layer from the steel specimens. Then the specimens were rinsed with ethanol and deionized water, and finally dried. The corrosive medium was 0.5 M H_2SO_4 prepared by using analytical grade reagents with deionized water. [AEIM]Br and [AHIM]Br shown as Fig. 1 were purchased from Lanzhou Greenchem ILS, LICP. CAS. China, which were used as test inhibitors in the concentration range of 1–10 mM. Moreover, the 0.5 M H_2SO_4 solution in the absence of inhibitors was taken as the blank for comparison.

2.2. Weight loss measurement

Some 250 mL glass beakers placed in a water thermostat were used to perform the weight loss test. Freshly polished steel specimens were precisely weighted and immersed in 0.5 M H_2SO_4 solution

with different concentrations of inhibitors for 20 h in triplicate at 298 K, respectively. After that, the X70 steel specimens were charily withdrawn, carefully rinsed in 0.1 M HCl, ultrapure water and acetone, then dried and weighted. The mean corrosion rates were calculated by the weight loss of each specimen and immersion time.

2.3. Electrochemical measurement

Electrochemical approaches were accomplished through a three-electrode system using a CHI 660E electrochemical station. Saturated calomel electrode (SCE) and Pt sheet (2.0 cm^2) were utilized as the reference electrode and the counter electrode, respectively. The X70 steel specimen was used as the working electrode. After the immersion in the corrosive solution, a stable system was obtained after 20 min monitoring of its open circuit potential (OCP). Afterwards, electrochemical impedance spectroscopy (EIS) was recorded at OCP in 100 kHz to 0.01 Hz frequency range with 5 mV peak amplitude AC signal. Finally, the polarization curves were performed at a scan rate of 1 mV/s and in the range of −250 mV to −250 mV of OCP.

2.4. SEM analysis

Scanning electron microscope (SEM) was applied to observe the surface morphology of X70 steel specimens after immersion in 0.5 M H_2SO_4 solution in the absence and presence of 10 mM investigated inhibitors for 8 h at 298 K.

2.5. Calculation details

The Forcite module in Material Studio was used to explore the interaction between investigated inhibitors and the Fe (110) surface. The molecular dynamics (MD) simulation was performed at 298 K, canonical ensemble (NVT), with a time step of 1.0 fs and simulation time of 300 ps. The effect of H_2O molecules were also considered.

3. RESULTS AND DISCUSSION

3.1. Potentiodynamic polarization curves

Fig. 2 shows polarization curves of X70 steel in 0.5 M H_2SO_4 solution with and without different concentrations of the studied inhibitors at 298 K. It can be seen that with the addition of [AEIM]Br and [AHIM]Br, the polarization curves shift obviously to lower current densities, and this inhibition effect is improved with the increase of their concentration. Besides, polarization curves of [AHIM]Br are lower than those of [AEIM]Br, which indicates a better inhibition performance. For [AEIM]Br and low concentrations of [AHIM]Br, only the cathodic part of polarization curves was

suppressed, indicating that these compounds mainly reduce cathodic hydrogen evolution thus prevent X70 steel from corrosion [15]. Particularly, cathodic and anodic part of polarization curves was both suppressed when the concentration of [AHIM]Br reach up to 10 mM. This reveals that [AHIM]Br acts as a cathodic-type inhibitor at low concentration, whereas [AHIM]Br experienced a transition from cathodic to mixed-type inhibitor with increasing its concentration.

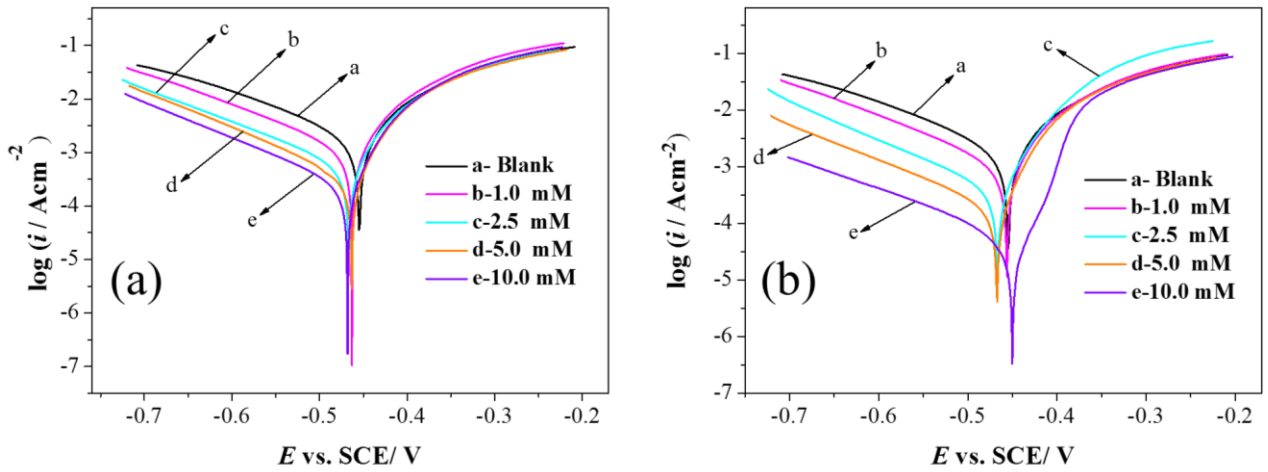

Figure 2. Polarization curves of X70 steel in 0.5 M H_2SO_4 solution in the absence and presence of various concentrations of (a)[AEIM]Br and (b)[AHIM]Br at 298K.

It is also can be seen that the addition of these inhibitors does not have a significant effect on the slope, revealing that these compounds does not change the reaction mechanism [16, 17].

The electrochemical parameters, including E_{corr} (corrosion potential), i_{corr} (corrosion current density), β_a (anodic polarization slope), β_c (cathodic polarization slope), η (inhibition efficiency) were calculated and listed in Table 1. The inhibition efficiency is defined as follows:

$$\eta(\%) = (1 - \frac{i_{corr}}{i_{corr,0}}) \times 100 \qquad (1)$$

where $i_{corr,0}$ and i_{corr} show unprotected and protected current densities of the steel electrode in the 0.5 M H_2SO_4 solution, respectively.

Table 1. The Potentiodynamic polarization parameters for X70 steel in 0.5 M H_2SO_4 solution in the absence and presence of diverse concentrations of two inhibitors

Inhibitor	C (mM)	E_{corr} (mV)	i_{corr} (mA cm^{-2})	β_c (mV dec^{-1})	β_a (mV dec^{-1})	η (%)
[AEIM]Br	0	–459	1.748	153.5	120.2	/
	1.0	–463	1.189	153.8	111.2	31.98
	2.5	–467	0.6961	155.0	103.8	60.18
	5.0	–463	0.3711	138.7	102.1	78.77
	10.0	–468	0.2386	145.8	95.27	86.35
[AHIM]Br	0	–459	1.748	153.5	120.2	/
	1.0	–456	1.089	152.8	113.1	37.70
	2.5	–465	0.4289	151.6	76.92	75.46
	5.0	–467	0.1912	155.3	54.98	89.06
	10.0	–450	0.0279	161.5	31.61	98.40

As seen in Table 1 that i_{corr} values decrease with the addition of two inhibitors. The values of i_{corr} continue to reduce and the inhibition efficiencies that calculated from i_{corr} increase with incremental concentration of these compounds. Remarkably, [AHIM]Br has the lower i_{corr} values and higher η values than [AEIM]Br. For [AEIM]Br, the value of η reach up to 86.35% at 10 mM, while 98.40% is obtained for [AHIM]Br at same condition.

3.2. EIS measurement

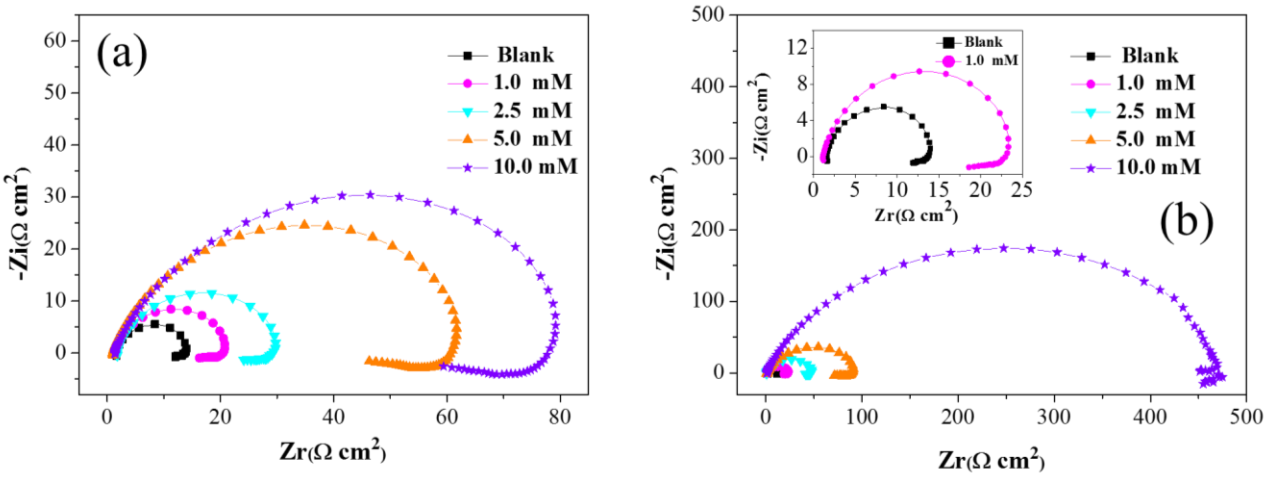

Figure 3. Nyquist impedance curves recorded for X70 steel electrode in 0.5 M H_2SO_4 solution without and with various concentrations of (a)[AEIM]Br and (b)[AHIM]Br at 298 K.

Nyquist plots of X70 steel specimens with and without various concentrations of [AEIM]Br and [AHIM]Br in 0.5 M H_2SO_4 are shown in Fig. 3. Nyquist plots can be regarded as two parts. The one is a capacitive loop at high frequency, which is related to the charge transfer and double layer behavior [18]. The another is an inductive loop at low frequency, which is due to the relaxation process of adsorbed particles on the steel surface [19]. Moreover, it can be clearly seen that diameters of Nyquist plots increase with the addition and increase of both inhibitors as compared to the diameter in blank specimen, revealing that the corrosion of steel was effectively inhibited. It is obvious that the shape of the Nyquist plots almost keep the same with different concentrations of these organic compounds, which indicates that the addition of studied compounds change the corrosion mechanism slightly and inhibit corrosion by enhancing the values of charge transfer resistance through adsorption ability [20, 21].

The used equivalent electric circuit is shown in Fig. 4. The circuit consists of solution resistance (*R*s), charge-transfer resistance (R_{ct}), constant phase element (*CPE*), and inductive elements (L and R_L). The *CPE* denotes C_{dl} (double layer capacitance), which can be calculated as follows [22]:

$$C_{dl} = Y_0 \left(2\pi f_{max}\right)^{n-1} \quad (2)$$

where Y_0 is the magnitude of the *CPE*, , f_{max} represents the frequency at the maximum value of the imaginary component of the impedance spectra. *n* is the deviation parameter in regard to phase shift.

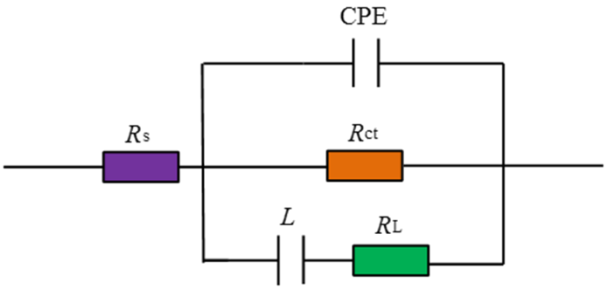

Figure 4. The equivalent circuits used for fitting the EIS data.

Table 2. Impedance parameters of X70 steel in 0.5 M H_2SO_4 solution in the absence and presence of different concentrations of [AEIM]Br and [AHIM]Br

Inhibitor	C (mM)	R_s (Ω cm^2)	*CPE*		C_{dl} (μF cm^{-2})	R_{ct} (Ω cm^2)	L (Ω cm^2)	R_L (Ω cm^2)	η (%)
			Y_0 ($\times 10^{-6}$ $S\,s^n$ cm^{-2})	n					
[AEIM]Br	0	1.56	203.7	0.91	114.3	13.47	20.48	75.60	/
	1.0	1.41	185.7	0.89	93.36	19.47	61.93	94.67	30.92
	2.5	1.76	166.4	0.87	75.69	28.21	95.51	154.9	52.25
	5.0	1.09	189.0	0.84	83.58	61.79	257.6	263.1	78.20
	10.0	1.35	238.6	0.80	92.91	81.02	289.6	300.9	83.37
[AHIM]Br	0	1.60	203.7	0.91	114.3	13.47	20.48	75.60	/
	1.0	1.20	165.1	0.88	77.98	22.23	74.64	118.1	39.41
	2.5	1.48	150.1	0.85	64.07	43.37	124.2	284.2	68.94
	5.0	1.30	112.6	0.84	48.29	90.80	458.3	430.3	85.17
	10.0	1.70	58.73	0.80	24.69	518.8	1115	0.001	97.40

The relevant impendence parameters values obtained from EIS are listed in Table 2. The inhibition efficiencies are determined by,

$$\eta(\%) = (1 - \frac{R_{ct,0}}{R_{ct}}) \times 100 \qquad (3)$$

It can be seen that the values of R_{ct} are much higher for inhibited conditions as compared to the R_{ct} value of uninhibited condition, manifesting the formation of inhibitor-adsorption film of [AEIM]Br and [AHIM]Br on steel surface, inhibiting the process of charge transfer. On the contrary, the values of C_{dl} display a decline tendency with the growing concentration of these compounds, which could be attributed to the gradually absorbed organic molecules, resulting to the increased thickness of electric double films or decrease in the values of dielectric constants [23]. Accordingly, for [AEIM]Br, the η value reached up to 83.37% at 10 mM from 30.92% at 1 mM, while [AHIM]Br has better inhibition performance with the η value of 97.40% at 10 mM and 39.41% at 1 mM. The obtained inhibition efficiencies agrees well with those calculated from polarization test, revealing that the addition of studied compounds enhanced corrosion resistance of steel in 0.5 M H_2SO_4 solution.

3.3. Weight loss study

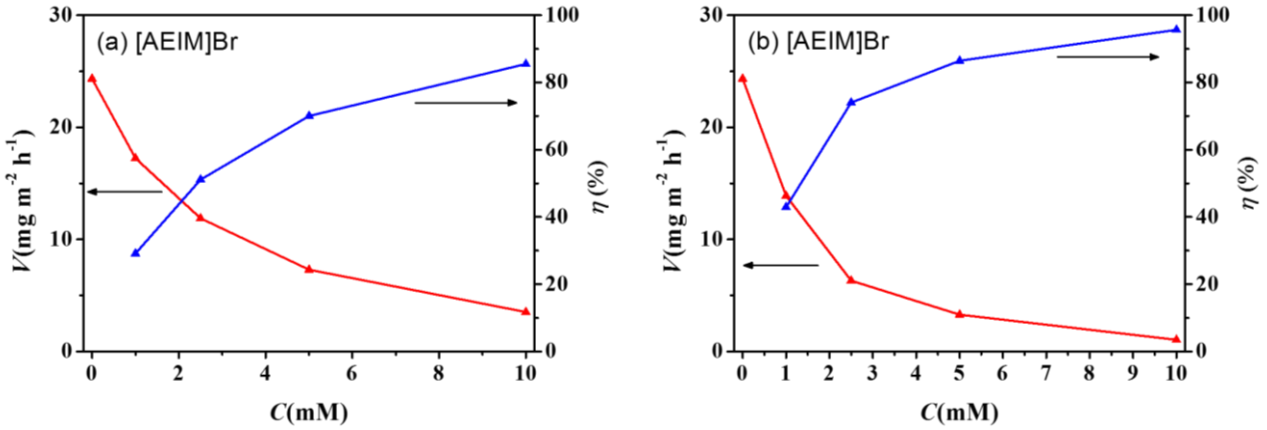

Figure 5. The weight loss graph of X70 steel in 0.5 M H_2SO_4 solution without and with various concentrations of (a)[AEIM]Br and (b)[AHIM]Br at 298 K.

The inhibition action of [AEIM]Br and [AHIM]Br at various concentrations on corrosion of X70 steel was investigated by weight loss measurement at 298 K after 20 h immersion. The relevant corrosion rate (v, mg m^{-2} h^{-1}) and inhibition efficiency (η) are calculated as follows and shown in Fig. 5.

$$v = \frac{W_0 - W}{St} \quad (4)$$

$$\eta(\%) = \frac{v_0 - v}{v_0} \times 100 \quad (5)$$

where S is the total sample surface area, t is the immersion time, W_0 and W are the weight of samples before and after exposure to corrosive solution, respectively, v_0 and v are the corrosion rates of steel samples without and with inhibitor, respectively.

As seen in Fig. 5, for each compound, the corrosion rates decrease and inhibition efficiencies increase with increasing concentration. Particularly, the lower corrosion rates and higher inhibition efficiencies were obtained for [AHIM]Br than those from the [AHIM]Br. This observation indicates that both compounds could adsorbed onto steel surface and thus inhibit steel corrosion in 0.5 H_2SO_4 solution, while [AHIM]Br have a superior inhibitive ability.

3.4. Adsorption isotherm study

The interaction between the metal surface and organic inhibitor can be very well understood in terms of the adsorption isotherm. In this work, several classical adsorption isotherms were used to fit the results obtained from weight loss measurement of the organic compound [24-26].

$$\frac{\theta}{1-\theta} = K_{ads}C \quad \text{(Langmiur isotherm)} \quad (6)$$

$$\left(\frac{\theta}{1-\theta}\right)\exp(2a\theta) = K_{ads}C \quad \text{(Frumkin isotherm)} \quad (7)$$

$$\exp(-2a\theta) = K_{ads}C \quad \text{(Temkin isotherm)} \quad (8)$$

where θ, the degree of the coverage, is defined as $\eta/100$, C is the concentration of the compound, K_{ads} is the equilibrium constant of adsorption process of the compound.

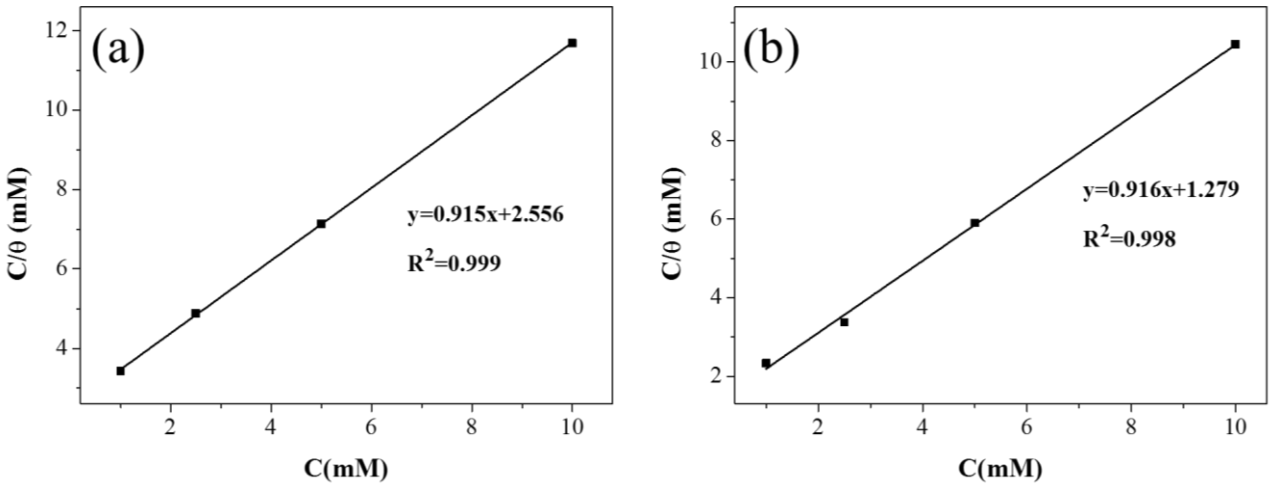

Figure 6. The Langmuir adsorption isotherms of (a)[AEIM]Br and (b)[AHIM]Br on steel surface in the test solution at 298 K.

The Langmuir adsorption isotherms of (a)[AEIM]Br and (b)[AHIM]Br on steel surface in the test solution at 298 K are shown in Fig. 6. The linear regression coefficients (R^2) of the straight line in Fig. 6 are 0.999 and 0.998, which shows that the linearity of the fitted straight line is good, indicating the adsorption of these compounds on the surface of X70 steel follows Langmuir adsorption isotherm. As shown in Fig. 6(a-b), the relationship between C and C/θ complies straight lines with intercept of $1/K$. The standard adsorption free energy (ΔG^0_{ads}) can be calculated by [26],

$$\Delta G^0_{ads} = -RT\ln(55.5K_{ads}) \quad (9)$$

here, T is the absolute temperature (K) and R is the molar gas constant (8.314 J mol^{-1} K^{-1}).

The calculated values of ΔG^0_{ads} are −24.74 kJ/mol for [AEIM]Br , −26.47 kJ/mol for [AHIM]Br, respectively. The negative sign of ΔG^0_{ads} demonstrates that the adsorption of these organic compounds on the steel surface is a spontaneous process [27]. It is generally believed that this adsorption behavior is the result of co-adsorption of physical and chemical adsorption and belongs to mixed adsorption when the value of ΔG^0_{ads} is between −40 kJ/mol and −20 kJ/mol [28]. Therefore, it can be concluded that both studied compounds on steel surface in present study is mixed adsorption between physisorption and chemisorption.

3.5. SEM observation

Fig. 7 shows SEM images of X70 steel after immersion in 0.5 H_2SO_4 solution in absence and presence of 10 mM studied inhibitors after 8 h at 298 K. As seen in Fig. 7a, the steel surface is badly damaged due to the aggressive attack from H_2SO_4 solution.

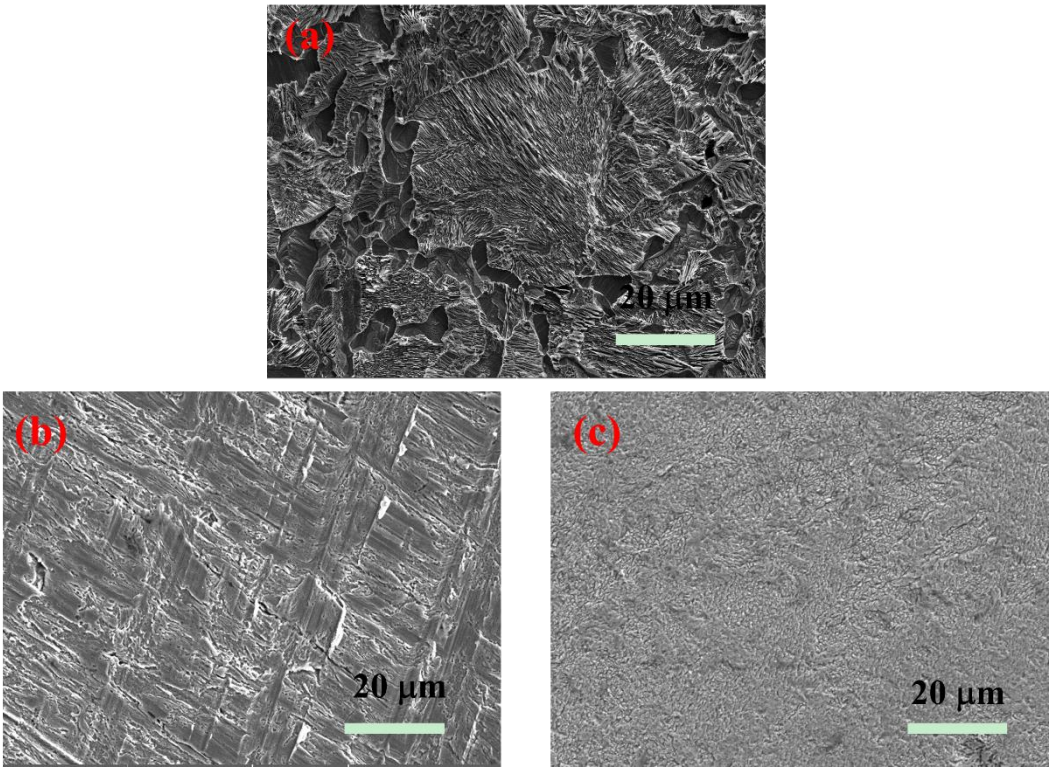

Figure 7. The X70 steel surfaces after immersion in 0.5 M H_2SO_4 solution (a) without and with 10 mM (b) [AEIM]Br or (c) [AHIM]Br for 8 h at 298K.

With the addition of [AEIM]Br and [AHIM]Br respectively, the X70 steel surfaces are relatively smooth and less damaged or corroded. In particular, the steel surface protected by [AHIM]Br (Fig. 7c) is smoother than that prevented by [AEIM]Br (Fig. 7b), which can furtherly confirm the better inhibition action of [AHIM]Br than [AEIM]Br.

3.6. Molecular dynamics simulation

MD simulation was performed to further investigating the interaction between studied compounds and the steel surface, Figs. 8 and 9 show the equilibrium adsorption configuration of studied inhibitor compounds on Fe (110) surface without and with H_2O molecules, respectively. Whatever the addition of water molecules, it is clearly seen that the both compounds are almost parallel with the surface of Fe (110). In this condition, the chemical bond could occur through donation of the lone pair of the heteroatoms to the Fe atoms [29, 30]. Besides, the parallel mode of [AHIM]Br than [AEIM]Br can effectively decrease contact area between the steel surface and aggressive particles, consequently reduce aggressive attack to steel substrate. In particular, bigger molecule [AHIM]Br can provide larger protective surface than the other one, which could denote to a better inhibitive ability.

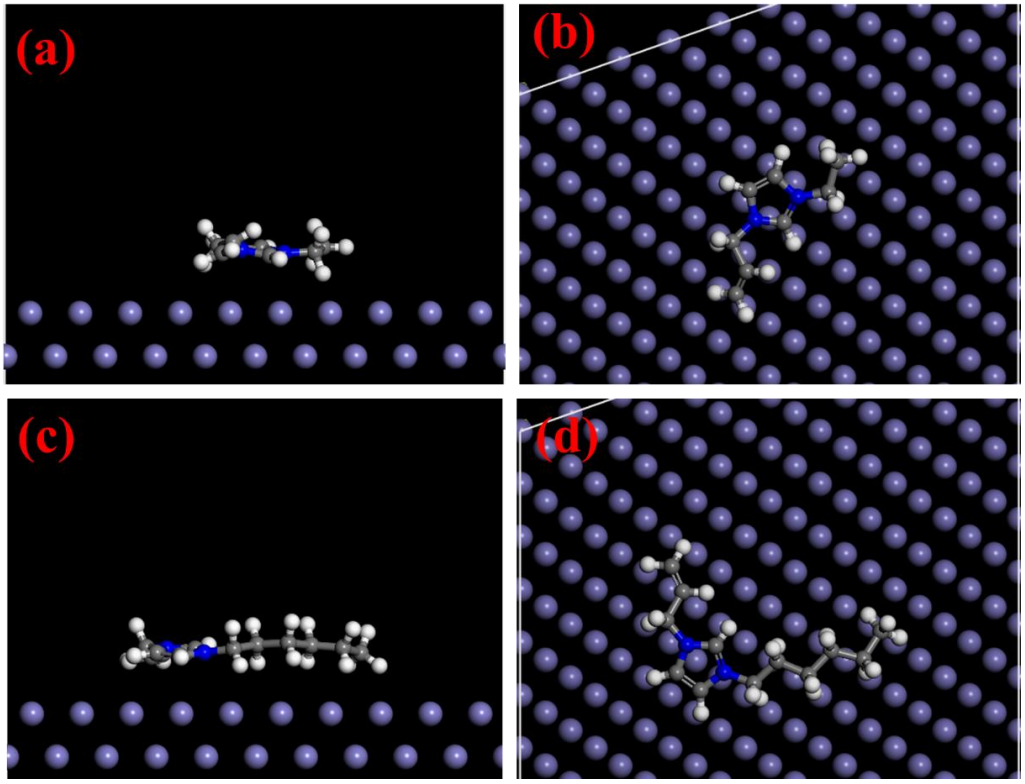

Figure 8. The adsorption equilibrium configurations for the studied compounds [AEIM]Br, (a) side view, (b) side view, and [AHIM]Br (c) side view, (d) top view, on Fe (110) surface without consideration of H_2O molecules.

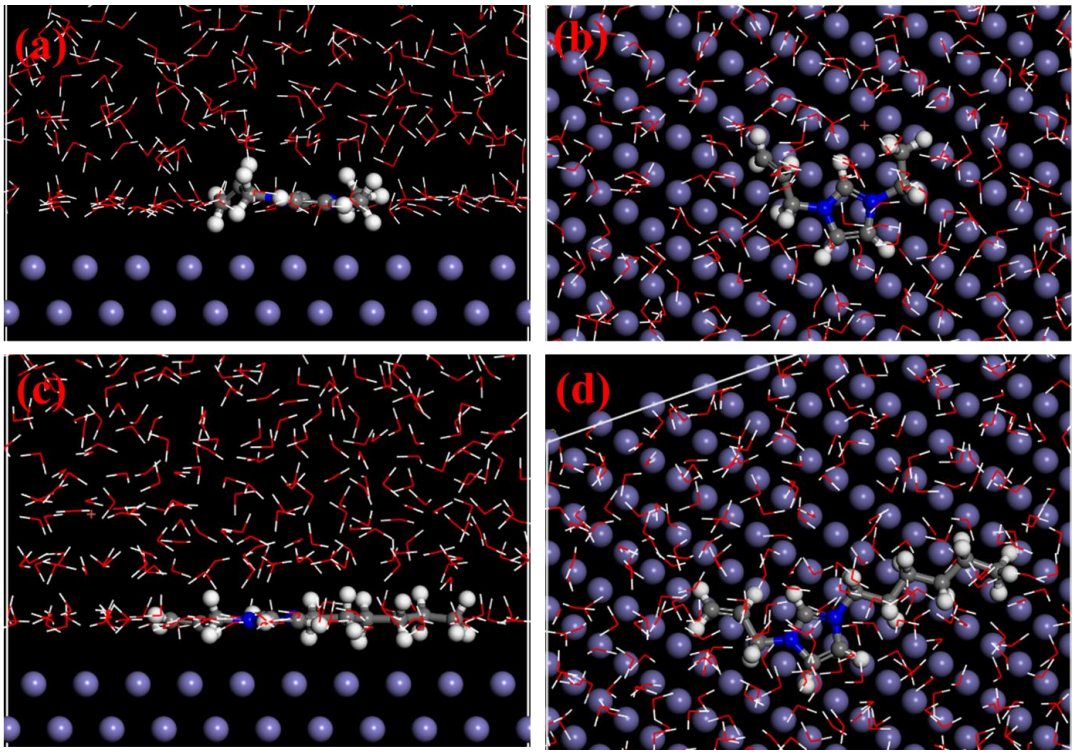

Figure 9. The adsorption equilibrium configurations for the studied compounds [AEIM]Br, (a) side view, (b) side view, and [AHIM]Br (c) side view, (d) top view, on Fe (110) surface with consideration of H_2O molecules.

Furtherly, the interaction energy ($E_{interact}$) between inhibitor molecules and the steel surface were also calculated. In the system without H_2O molecules, the obtained values of $E_{interact}$([AEIM]Br) and $E_{interact}$([AHIM]Br) were 86.4 and 144.7 kcal/mol, respectively. In the system containing H_2O molecules, $E_{interact}$([AEIM]Br) = 238.8 kcal/mol, $E_{interact}$([AHIM]Br) = 297.8 kcal/mol. Although the existence of water molecules influence the interaction energy values, the two values follow the same trend. Generally, the high value of $E_{interact}$ means that the inhibitor can adsorb onto the steel surface easily and strongly [31, 32]. In present study, the higher value of [AHIM]Br confirms its superior inhibition performance than [AEIM]Br calculated from the experimental results above.

4. CONCLUSIONS

Two imidazolium-based ILs with different chain lengths were investigated on corrosion resistance for X70 steel in 0.5 M sulphuric acid. The following conclusions can be drawn:

(1) Weight loss experiment reveal that [AHIM]Br has a better inhibitive ability for X70 steel corrosion than [AEIM]Br in aggressive medium and the inhibition performance increases with the augment of concentration.

(2) Electrochemical results agrees well with the weight loss experiment and indicates that [AEIM]Br is a cathodic-type inhibitor. On the other hand, low concentration of [AHIM]Br is a cathodic inhibitor, while high concentration makes it mixed-type.

(3) SEM confirmed the inhibitive order of studied inhibitors.

(4) Adsorption isotherm study proves that adsorption of two inhibitors is a spontaneous mixed physical and chemical adsorption obeying Langmuir adsorption isotherm.

(5) The MD study is consistent with the experimental data and provide evidence for the mechanism of inhibitors. The larger protective area from [AHIM]Br bringing its better inhibitive ability than [AEIM]Br.

References

1. A. Dutta, S.K. Saha, U. Adhikari, P. Banerjee, D. Sukul, *Corros. Sci.*, 123 (2017) 256-266.
2. F. Branzoi, V. Branzoi, *Inter. J. Electrochem. Sci.*, 12 (2017) 7638-7658.
3. Z. Xiao, H. Wu, G. Liang, D. Zhan, *Inter. J. Electrochem. Sci.*, 12 (2017) 10969-10980.
4. X. Zheng, M. Gong, C. Liu, *Inter. J. Electrochem. Sci.*, 12 (2017) 5553-5566.
5. N. Kumari, P.K. Paul, L. Gope, M. Yadav, *J. Adhesion Sci. Tech.*, 31 (2016) 1524-1544.
6. X. Su, C. Lai, L. Peng, H. Zhu, L. Zhou, *Inter. J. Electrochem. Sci.*, 11 (2016) 4828-4839.
7. G. Sığırcık, D. Yildirim, T. Tüken, *Corros. Sci.*, 120 (2017) 184-193.
8. E. Gutiérrez, J.A. Rodríguez, J. Cruz-Borbolla, J.G. Alvarado-Rodríguez, P. Thangarasu, *Corros. Sci.*, 108 (2016) 23-35.
9. K. Azzaoui, E. Mejdoubi, S. Jodeh, A. Lamhamdi, E. Rodriguez-Castellón, M. Algarra, A. Zarrouk, A. Errich, R. Salghi, H. Lgaz, *Corros. Sci.*, 129 (2017) 70-81.
10. G.L.F. Mendonça, S.N. Costa, V.N. Freire, P.N.S. Casciano, A.N. Correia, P.d. Lima-Neto, *Corros. Sci.*, 115 (2017) 41-55.
11. Y. Qiang, S. Zhang, B. Tan, S. Chen, *Corros. Sci.*, 133 (2018) 6-16.

12. L. Luo, S. Zhang, Y. Qiang, N. Chen, *Inter. J. Electrochem. Sci.*, 11 (2016) 8177-8192.
13. N.X. Chen, S.T. Zhang, Y.J. Qiang, S.Y. Xu, X.L. Ren, *Inter. J. Electrochem. Sci.*, 11 (2016) 7230-7241.
14. Y. Qiang, S. Zhang, L. Guo, X. Zheng, B. Xiang, S. Chen, *Corros. Sci.*, 119 (2017) 68-78.
15. H. Bi, G.T. Burstein, B.B. Rodriguez, G. Kawaley, *Corros. Sci.*, 102 (2016) 510-516.
16. Y. Qiang, S. Zhang, S. Xu, W. Li, *J. Colloid Interf. Sci.*, 472 (2016) 52-59.
17. O. Olivares-Xometl, E. Álvarez-Álvarez, N.V. Likhanova, I.V. Lijanova, R.E. Hernández-Ramírez, P. Arellanes-Lozada, J.L. Varela-Caselis, *J. Adhesion Sci. Tech.*, 32 (2017) 1092-1113.
18. S.A. Umoren, A. Madhankumar, *J. Mol. Liq.*, 224 (2016) 72-82.
19. G. Karthik, M. Sundaravadivelu, *J. Adhesion Sci. Tech.*, 31 (2016) 530-551.
20. Z. Tao, S. Zhang, W. Li, B. Hou, *Corros. Sci*., 51 (2009) 2588-2595.
21. G. Khan, W.J. Basirun, S.N. Kazi, P. Ahmed, L. Magaji, S.M. Ahmed, G.M. Khan, M.A. Rehman, *J. Colloid Interf. Sci.*, 502 (2017) 134-145.
22. P. Singh, E.E. Ebenso, L.O. Olasunkanmi, I.B. Obot, M.A. Quraishi, *J. Phys. Chem. C*, 120 (2016) 3408-3419.
23. Y. Qiang, S. Zhang, S. Yan, X. Zou, S. Chen, *Corros. Sci.*, 126 (2017) 295-304.
24. A. Yousefi, S. Javadian, J. Neshati, *Ind. Eng. Chem. Res.*, 53 (2014) 5475-5489.
25. Y.J. Qiang, S.T. Zhang, S.Y. Xu, L.L. Yin, *RSC Adv.*, 5 (2015) 63866-63873.
26. G. Ji, S. Anjum, S. Sundaram, R. Prakash, *Corros. Sci.*, 90 (2015) 107-117.
27. C. Verma, A. Singh, G. Pallikonda, M. Chakravarty, M.A. Quraishi, I. Bahadur, E.E. Ebenso, *J. Mol. Liq.*, 209 (2015) 306-319.
28. Y. Qiang, S. Zhang, L. Guo, S. Xu, L. Feng, I.B. Obot, S. Chen, *J. Clean. Prod.*, 152 (2017) 17-25.
29. M.B. Radovanović, M.M. Antonijević, *J. Adhesion Sci., Tech.*, 31 (2016) 369-387.
30. S.A. Umoren, Z.M. Gasem, I.B. Obot, *Ind. Eng. Chem. Res.*, 52 (2013) 14855-14865.
31. D.K. Yadav, M.A. Quraishi, *Ind. Eng. Chem. Res.*, 51 (2012) 14966-14979.
32. Y. Qiang, S. Zhang, S. Xu, L. Guo, N. Chen, I.B. Obot, *Inter. J. Electrochem. Sci.*, 11 (2016) 3147-3163.